# Interfacial structures of whey protein isolate (WPI) and lactoferrin on hydrophobic surfaces in a model system monitored by quartz crystal microbalance with dissipation (QCM-D) and their formation on nanoemulsions

Food Hydrocolloids 56 (2016) 150–160

Contents lists available at ScienceDirect

Food Hydrocolloids

journal homepage: www.elsevier.com/locate/foodhyd

# Interfacial structures of whey protein isolate (WPI) and lactoferrin on hydrophobic surfaces in a model system monitored by quartz crystal microbalance with dissipation (QCM-D) and their formation on nanoemulsions

Anges Teo [a, b], Simone Dimartino [c, d], Sung Je Lee [a, *], Kelvin K.T. Goh [b], Jingyuan Wen [e], Indrawati Oey [f], Sanghoon Ko [g], Hae-Soo Kwak [g]

[a] School of Food and Nutrition, Massey University, Auckland, New Zealand
[b] School of Food and Nutrition, Massey University, Palmerston North, New Zealand
[c] Department of Chemical and Process Engineering, University of Canterbury, Christchurch, New Zealand
[d] Biomolecular Interaction Centre, University of Canterbury, Christchurch, New Zealand
[e] School of Pharmacy, University of Auckland, New Zealand
[f] Department of Food Science, University of Otago, Dunedin, New Zealand
[g] Department of Food Science and Technology, Sejong University, Seoul, Korea

ARTICLE INFO

*Article history:*
Received 18 August 2015
Received in revised form
20 November 2015
Accepted 2 December 2015
Available online 10 December 2015

*Keywords:*
Nanoemulsions
Interfacial structures
Protein interactions
Whey protein isolate (WPI)
Lactoferrin
Quartz crystal microbalance with dissipation (QCM-D)

ABSTRACT

In this work, the interactions between two oppositely charged proteins in solution, namely whey protein isolate (WPI) and lactoferrin, were investigated for uses in nanoemulsions. ζ-potential and turbidity measurements indicated that these two proteins interact strongly via electrostatic attraction at pH 6. Quartz crystal microbalance with dissipation (QCM-D) was employed to study the adsorption behaviour and the formation of different interfacial structures of the two proteins onto a model hydrophobic surface that mimics the interface of an oil droplet in emulsions. Sequential addition of WPI and lactoferrin (or vice versa) formed thin and rigid protein bi-layers (8–10 nm). However, a viscous and thick surface layer (101 nm) was formed by the protein complex using a mixture of WPI and lactoferrin. High pressure homogenization and solvent evaporation were then used to replicate the QCM-D results on real nanoemulsion systems. Sequential adsorption of WPI and lactoferrin created bi-layered nanoemulsions with stable and relatively small droplets (90 nm in diameter). In contrast, the sequential adsorption of lactoferrin and WPI as well as the use of a mixture of WPI and lactoferrin (mixed layer) resulted in large aggregates with poor stability. This study provided insights into the stability of nanoemulsions influenced by structural features of interfacial layers based on two oppositely charged protein molecules.


## 1. Introduction

Oil-in-water (O/W) nanoemulsions are defined as emulsions containing oil droplets with size in the range of 10–100 nm in diameter (Lee, Choi, Li, Decker, & McClements, 2011; Lee & McClements, 2010;). The small droplet size of nanoemulsions has a number of advantages including high stability against droplet aggregation and coalescence, incorporation of bioactive compounds into clear and transparent solutions and enhancement of solubility and bioavailability of poorly soluble drugs (McClements & Rao, 2011; Tiwari & Takhistove, 2012; Weiss, Gaysinsky, Davidson, & McClements, 2009).

Like conventional emulsions containing large oil droplets (0.1–100 μm), the structure and composition of the oil-water interface of nanoemulsions can be manipulated to form emulsions with better performance and novel functionalities as microencapsulation systems of bioactive compounds (Skirtach, Yashchenok, & Möhwald, 2011; Trojer et al., 2015; Trojer, Nordstiema, Nordin, Nydén, & Holmberg, 2013). This can be achieved by depositing oppositely charged biopolymers at the interface of oil droplets using an electrostatic layer by layer (LBL) deposition method to form multi-layer emulsions (Bouyer,

* Corresponding author.
*E-mail address:* s.j.lee@massey.ac.nz (S.J. Lee).

http://dx.doi.org/10.1016/j.foodhyd.2015.12.002
0268-005X/

Mekhloufi, Rosilio, Grossiord, & Agnely, 2012; Guzey & McClements, 2006; Sukhorukov, Caruso, Davis, & Möhwald, 1998;). Alternatively, electrostatic complexes of two oppositely charged biopolymers can be used to form mixed layer emulsions (Bouyer et al., 2012; Tokle, Decker, & McClements, 2012). Examples of multi-layer and mixed layer emulsions have been reported in the literature, e.g. caseinate/sodium alginate multi-layer emulsions (Pallandre, Decker, & McClements, 2007); β-lactoglobulin/lactoferrin multi-layer emulsions (Ye & Singh, 2007); β-lactoglobulin/lactoferrin multi-layer and mixed layer emulsions (Tokle et al., 2012), and WPI/pectin mixed layer emulsions (Mao, Boiteux, Roos, & Miao, 2014). These studies have shown that modification of interfacial properties can influence the stability of emulsions under environmental stresses (such as pH, ionic strength and temperature) and affect chemical and oxidative stability of encapsulated components in the oil droplets. However, majority of these studies have been focused on conventional emulsions containing relatively large droplet size, and the mechanism underlying the complex formation and the interfacial structure of small oil droplets has yet to be fully understood. This is interesting because the interfacial characteristic of nanoemulsions is different from conventional emulsions. The small oil droplets of nanoemulsions are being surrounded by a thicker interfacial layer whereas conventional emulsions have a thinner interfacial layer relative to their respective droplet size (McClements & Rao, 2011). As a result, the interfacial properties of nanoemulsions have a greater influence on the overall particle characteristics, such as physical stability, particle interactions and stability and digestibility of emulsions.

Formation of multi-layer interfaces involves species (e.g. weak polyelectrolytes) having different isoelectric points in a pH dependent process driven by electrostatic interactions (Guzey & McClements, 2006; Ye & Singh, 2007). In the case of micron sized emulsions, the composition and structure of the biomolecules adsorbed at the droplet surface can be determined by centrifugation followed by gel electrophoresis of the cream layer (Sarkar, Goh, Singh, & Singh, 2009; Ye & Singh, 2007). However, such protocol cannot be employed with nanoemulsions, which are characterised by kinetically stable small oil droplets that cannot be readily separated by centrifugal forces. The interfacial structures on nanoemulsions can be studied through indirect techniques such as surface plasmon resonance (SPR), quartz crystal microbalance with dissipation (QCM-D), atomic force microscopy (AFM), ellipsometry, dual polarisation interferometry, optical tensiometry and dilatational rheology (Boddohi, Almodóvar, Zhang, Johnson, & Kipper, 2010; Krivosheeva, Dėdinaitė, & Claesson, 2012; Lundin, Elofsson, Blomberg, & Rutland, 2010; Trojer, Mohamed, & Eastoe, 2013). Here, a model surface is used to mimic the oil droplet interface, allowing the monitoring of the adsorption of different layers and their resulting structural characteristics. For example, Berendsen, Güell, Henry, and Ferrando (2014) used SPR technique to study the formation of multi-layer emulsions with different interfacial structures, e.g. mono-layer, bi-layer and complex layer.

Interestingly, QCM-D has not been well used to study the interfacial structures of protein layers in emulsions. QCM-D is well-suited to measure surface adsorption and structural properties of adsorbed layers. In fact, the quartz crystals used in QCM-D measurements can be chemically modified to create a hydrophobic layer which can then be used to mimic the oil-water interface in real emulsions. In previous studies, gold coated quartz crystals used in the QCM-D experiments have been modified using an alkanethiol molecule (1-hexadecanethiol). This molecule has been used in the formation of a self-assembled monolayer (SAM) hydrophobic surface and contains a thiol group $(CH_3CH_2)_{14}CH_2SH$ that can be immobilised onto gold surfaces through a covalent bond (Ito, Arai, Hara, & Noh, 2009; Nováková, Oriňáková, Oriňák, Hvizdoš, & Fedorková, 2014). It has been shown that the formation of SAM of alkyl thiols containing $CH_3$ terminated groups is hydrophobic and that protein adsorption on the modified surfaces is driven by hydrophobic interactions (Lebec et al., 2013). This technique enables simultaneous measurement of the resonance frequency of an oscillating sensor and decay of the oscillation (i.e. dissipation) which are related to the amount of adsorbed layer and its viscoelastic properties, respectively (Höök et al., 2001; Liu & Kim, 2009; Lundin et al., 2010). This surface characterization technique has been successfully used to study adsorption of proteins and formation of multi-layers on different surfaces for biomedical and other applications (Chandrasekaran, Dimartino, & Fee, 2013; Craig, Bordes, & Holmberg, 2012; Lundin et al., 2010). Still, QCM-D has not been employed as a complementary technique to study protein adsorption at the O/W interface in emulsion systems.

In this study, the interactions of WPI and/or lactoferrin at an oil-water interface were studied in a model system by depositing aqueous protein solutions to a gold hydrophobic surface using QCM-D technique. This model system was used to simulate the adsorption of protein on the hydrophobic surface of oil droplets in aqueous solution. QCM-D was employed to measure the extent of protein adsorption and to determine the formation of different interfacial structures. Nanoemulsions with similar interfacial structures were also prepared in parallel and the results from the two sets of experiments compared. This study provides valuable information on the structural design of layered nanoemulsions.

## 2. Materials and methods

### 2.1. Materials

Whey protein isolate (WPI) (Alacen™ 895) containing 93.9% protein, 0.3% fat, 1.5% ash and 4.7% moisture was supplied by Fonterra Co-operative Group Limited, New Zealand. Lactoferrin powder containing 98.8% protein (of which 92.8% was lactoferrin), 0.7% ash and 0.4% moisture was obtained from Tatua Co-operative Dairy Company, Morrinsville, New Zealand. 1-hexadecanethiol (≥95% GC) was purchased from Sigma Chemical Co. (St. Louis, MO, USA). Ammonia (25%) and hydrogen peroxide (30%) were purchased from Sigma Aldrich (Sydney, Australia). Corn oil was purchased from a local supermarket (Davis Trading, Palmerston North, New Zealand). Ethyl acetate (HPLC grade) was purchased from Fischer Scientific (New Jersey, USA). Hydrochloric acid, sodium hydroxide and sodium azide were of analytical grade and purchased from Thermo Fisher Scientific (Victoria, Australia) or BDH Chemicals (Poole, England).

### 2.2. Preparation of protein solutions

Protein solutions containing 1% (w/w) WPI or lactoferrin were prepared in Milli-Q water (Millipore, 18.2 MΩ cm at 25 °C) under gentle stirring for at least 3 h at room temperature. The pH of protein solutions was adjusted with HCl or NaOH solutions to the pH value required in the experiment (ranging from 2 to 10). A mixture of WPI and lactoferrin was also prepared by mixing equal volumes of both protein solutions at pH 6.

### 2.3. Analysis of protein solutions

#### 2.3.1. Electrical charge (ζ-potential) measurements

The ζ-potentials of protein solutions and protein mixtures were determined in disposable folded capillary cells (Model DTS1070) using a Malvern Zetasizer Nano ZS (Malvern Instruments, Worcestershire, UK). The samples were analysed at 25 °C in triplicate without further dilution. The ζ-potential was calculated from the

measured electrophoretic mobility of oil droplets using the Smoluchowski model (Zetasizer Software, Version 7.10, Malvern Instruments, Worcestershire, UK).

#### 2.3.2. Turbidity measurements

The optical density (O.D.) of individual protein solutions and protein mixtures of WPI and lactoferrin was measured at 600 nm using a UV-visible spectrophotometer (SPECTROstar$^{Nano}$, BMG LABTECH GmbH, Ortenberg, Germany) in a 1 cm path length optical cell against a water reference.

### 2.4. Quartz crystal microbalance with dissipation (QCM-D) measurements

#### 2.4.1. Preparation of hydrophobic gold surfaces

AT-cut piezoelectric quartz crystals (Q-Sense, ATA Scientific, Tarren Point, NSW, Australia) coated with gold and having a fundamental frequency of 4.95 Hz were used. The gold sensors were cleaned with "Piranha" solution (a mixture of 5:1:1 ratio of Milli-Q water, 25% ammonia and 30% hydrogen peroxide) at 75 °C for 10 min and rinsed with hot Milli-Q water. The sensors were dried with nitrogen gas and placed in a UV/ozone chamber (Bio-Force Nanosciences, USA) for 10 min.

After cleaning and drying the sensors, the gold surface was rendered hydrophobic by introducing a self-assembled monolayer (SAM) as per the protocol reported by Lebec et al. (2013) and Mivehi, Bordes, and Holmberg (2013). Briefly, the cleaned gold surface was immersed overnight in a solution of 2 mM hexadecanethiol in ethanol and then rinsed thoroughly with ethanol to remove unadsorbed hexadecanethiol. The contact angle of the modified sensor surface was measured using the drop analysis in Image J (Version 1.47, National Institutes of Health, USA).

#### 2.4.2. QCM-D experiment

Protein adsorption on the SAM hydrophobic surfaces was carried out using a QCM-D system (Q-Sense E4 system, Q-Sense, ATA Scientific, Tarren Point, NSW, Australia) equipped with a temperature controlled measuring chamber and a peristaltic pump (ISMATEC® IPC High Precision Multi channel Dispenser, IDEX Health & Science, Germany). Each QCM-D experiment started with pre-equilibration with Milli-Q water to obtain a signal baseline before addition of protein solutions. The test solutions were then fed to the SAM hydrophobic QCM-D sensors at a flow rate of 0.1 ml/min. All experiments were measured at 22 ± 2 °C.

Protein bi-layers were obtained at a given pH value in the range of 2–10 by successive addition of the individual protein solution until equilibrium, i.e. when stable frequency and dissipation signals were reached. Poorly adsorbed or unadsorbed proteins were removed by intermediate rinsing steps with Milli-Q water with the same pH as the protein solution. The adsorption of protein complex was studied at pH 6 by feeding the protein mixture until equilibrium, followed by a rinse with Milli-Q water.

#### 2.4.3. Data analysis of QCM-D results

In the QCM-D experiments, the changes in the resonance frequency and dissipation were recorded at several overtones and analysed to calculate the mass adsorbed using the Sauerbrey or the Kevin-Voigt model using Q-Tools$^{TM}$ software (version 3.0.12, Biolin Scientific AB, Sweden).

In the simplest case of a thin, homogeneous and rigidly adsorbed layer, the frequency shift of the oscillating quartz crystal is linearly related to the mass adsorbed on the crystal surface according to the Sauerbrey model (Sauerbrey, 1959):

$$\Delta m = -C\frac{\Delta f}{n} \quad (1)$$

where $\Delta m$ is the adsorbed mass, $\Delta f$ is the frequency shift at the overtone number, $n$ and $C$ is the mass sensitivity constant of the quartz crystal. For the 4.95 MHz sensor used in this study, the constant (C) is equal to 17.7 ng/cm$^2$ Hz (Malmström, Agheli, Kingshott, & Sutherland, 2007). The thickness of the adsorbed layer, $h_{eff}$, can be calculated from the following equation:

$$h_{eff} = \frac{\Delta m}{\rho_{eff}} \quad (2)$$

where $\rho_{eff}$ is the effective surface density of adsorbed protein layer.

However, when the adsorbed film displays strong viscoelastic properties, the Sauerbrey equation underestimates the actual mass adsorbed (Liu & Kim, 2009). In this case, the frequency and dissipation data collected at different overtones are modelled using the software based on the Kevin-Voigt model (Voinova, Rohahl, Jonson, & Kasemo, 1999). According to this model, the viscoelastic properties of the adsorbed protein layer and the QCM-D responses, $\Delta f$ (frequency shift) and $\Delta D$ (dissipation shift), can be expressed (Liu & Kim, 2009). In this case, the 5th, 7th and 9th overtones were used and the parameters of the fit for fluid viscosity and density were assumed to be 0.001 kg.ms and 1000 kg/m$^3$, respectively.

### 2.5. Preparation of nanoemulsions

Nanoemulsions were prepared by emulsification and solvent evaporation technique following the method reported by Lee et al. (2011) with some modifications. In this method, two different phases, denoted as organic phase and aqueous phase, were initially prepared separately and then mixed at an organic phase and aqueous phase ratio of 10:90 to produce nanoemulsions. The aqueous phase consisted of a 2% (w/w) protein solution (WPI or lactoferrin) or a protein mixture of WPI and lactoferrin (1:1 ratio) while the organic phase consisted of 90% (w/w) ethyl acetate and 10% (w/w) corn oil. The aqueous phase and organic phase were mixed together using a high shear mixer (Ultra Turrax® T25 Basic, IKA, Staufen, Germany) at 16,000 rpm for 2 min to form a coarse emulsion. The coarse emulsion was passed through a high-pressure homogeniser (M-110P, Microfluidics, Westwood, MA, USA) for 4 times at 12,000 psi (82.7 MPa) to produce a fine emulsion. There was a decrease in particle size of the coarse emulsion from around 1200 to 90 nm after microfluidisation. The fine emulsion was then treated for evaporation in a round bottom flask to remove ethyl acetate using a rotary evaporator (Buchi Rotavapor R-215, Vacuum Controller V850 and Heating Bath B-491, BUCHI Labortechnik AG, Flawil, Switzerland) operated at 50 °C with a vacuum pressure of 153 mbar for 20–25 min. The particle size of nanoemulsions was further decreased to 80 nm after evaporation. This resulted in the nanoemulsion droplets that were comprised entirely of corn oil. During evaporation, in addition to ethyl acetate, some water was also removed and this was adjusted by adding water back based on the mass balance of emulsion before and after solvent evaporation. . The nanoemulsions containing 1% (w/w) oil stabilised by WPI or lactoferrin or a mixture of them are denoted hereafter as primary nanoemulsions (or emulsions) with a single layer or mixed layer, respectively.

For bi-layer nanoemulsions, the WPI- or lactoferrin-stabilised primary nanoemulsions were mixed with an equal proportion of lactoferrin or WPI solution at pH 6. The resulting bi-layer nanoemulsions contained 0.5% (w/w) oil and are denoted as the secondary WPI-LF and LF-WPI nanoemulsions, respectively. The single

layer or mixed layer primary nanoemulsions were also diluted with water to make a final oil concentration of 0.5% (w/w). All emulsions were stored for 1 day at room temperature (20 ± 1 °C) before analysis.

### 2.6. Characterisation of nanoemulsions

#### 2.6.1. Droplet size and size distribution

The droplet size and size distribution of single layer nanoemulsions and WPI-LF nanoemulsions were measured by dynamic light scattering technique using a Malvern Zetasizer Nano ZS (Malvern Instruments Ltd, Worcestershire, UK) equipped with a helium/neon laser employing a wavelength of 633 nm and a backscattering angle of 173°. The emulsion samples were analysed without further dilution. The droplet size results were reported as Z-average mean diameter based on Stokes-Einstein equation. For sequential adsorption of lactoferrin and WPI or mixed layer emulsions containing relatively large droplets (>6 um) that could not be measured using the Malvern Zetasizer, they were measured using a Mastersizer instrument (Mastersizer 2000 Hydro MU, Malvern Instruments, Worcestershire, UK). A refractive index of 1.47 and 1.33 was used for the oil droplets and the dispersant medium, respectively and the sample was gently dispersed in water. The particle size was reported as the volume mean diameter, $d_{43} = \frac{\Sigma_i n_i d_i^4}{\Sigma_i n_i d_i^3}$, where $n_i$ is the amount of droplets with diameter $d_i$.

#### 2.6.2. Microscopy analysis

The microstructure of nanoemulsions was monitored by transmission electron microscopy (TEM). Sample preparation for TEM was carried out according to the method described by Gallier, Tate, and Singh (2013). Emulsion samples were injected into freshly made 3% agarose tubes (Hydragene Co. Ltd., Xiamen, China) and sealed at the end of tube with remaining agarose. The embedded samples in agarose tubes were fixed with 3% (w/w) glutaraldehyde in 0.1 M cacodylate buffer (Merck, Darmstadt, Germany) at pH 7.2 and subjected to a second fixture with 1% osmium tetraoxide (ProSciTech, Thuringowa, Australia) in the same buffer. The samples were dehydrated in a series of acetone washes consisting of 25% (v/v) acetone (15 min), 50, 75 and 90% (v/v) acetone (30 min each) and 100% acetone (30 min for 3 times) (Merck, Darmstadt, Germany). The samples were then immersed in a 1:1 ratio of acetone and resin (ProSciTech, Thuringowa, Australia) for overnight, then transferred to 100% resin for 52 h and finally embedded in a fresh 100% resin. The samples were polymerized at 63 °C for 48 h.

The embedded samples in resin blocks were trimmed using a glass knife on the ultramicrotome (Leica EM UC7, Heidelberg, Germany) and sliced to ultrathin sections using a diamond knife (Diatome, Hatfield, PA, USA). The thin sections of the embedded samples were placed on a copper grid using a Coat Quick "G" adhesive pen (Saiko, Japan) and stained with saturated uranyl acetate (BDH Chemicals, Poole, England) in 50% (w/w) ethanol (Merck, Darmstadt, Germany) followed by 0.25% (w/w) lead citrate (BDH Chemicals, Poole, England). Sections were then mounted in a specimen holder and inserted into the microscope cooled by liquid nitrogen. The samples were viewed using a transmission electron microscope (FEI Tecnai™ G2 Spirit BioTWIN, Czech Republic) operated at 60 kV and equipped with a $LaB_6$ filament. The TEM images were captured with a 2K × 2K Veleta camera (14 bit) (Olympus Soft Imaging Solutions GmbH, Münster, Germany).

### 2.7. Data analysis

All experiments were carried out at least in duplicates using freshly prepared samples. All statistical analysis was done using MS-Excel 2010 package. The results are reported as means and standard deviations.

## 3. Results and discussion

### 3.1. Characteristics of individual protein solution and protein mixture

The knowledge of the characteristics of aqueous solutions containing the proteins under investigation (i.e. WPI and lactoferrin) is fundamentally important to elucidate the structure of the resulting interfacial layer at the oil-water interface of nanoemulsions. The ζ-potential of proteins was measured at different pH values ranging from 2 to 10. As reasonably expected, the ζ-potential of WPI was positive at acidic pH and turned negative at basic pH (Fig. 1). The results obtained in this study were similar to a study on the effect of pH on the ζ-potential of protein solutions (e.g. β-lactoglobulin and/or lactoferrin) reported by Tokle et al. (2012). The point of zero charge (or isoelectric point, pI) for WPI was 4.9, a value matching previous results reported in the literatures (Berendsen et al., 2014; Salminen & Weiss, 2013). An increase in the turbidity of protein solutions containing WPI related to protein aggregation was apparent at pH close to the pI (pH 4.5–5.5) due to loss of electrostatic repulsion (Fig. 2). On the other hand, the pI of lactoferrin molecules was around 8.8 because of its high concentration of basic amino acids (Baker & Baker, 2005; Steijns & van Hooijdonk, 2000). The lactoferrin molecules were however stable to aggregation across the pH range studied with no noticeable change in solution turbidity even at the pI of the molecules (Fig. 2). It is known that lactoferrin contains amphiphilic moieties and exists as a mixture of positively charged monomers and negatively charged aggregates in the bulk solution (Mela, Aumaitrem, Williamson, & Yakubov, 2010). At pH below the pI, the lactoferrin is dominated by the monomers and are positively charged. As the pH approaches the pI, the monomers decrease and the aggregates increase. However, because the aggregates are negatively charged there are intra-molecular repulsive forces for the lactoferrin solution to remain clear which explains why lactoferrin solution is clear at the pI.

When the solution pH is at the intermediate range between the pI for WPI and lactoferrin, the two proteins possess opposite charge and will interact with each other through electrostatic forces. To assess the pH at which the two proteins would interact strongly, the ζ-potential of a mixture of WPI and lactoferrin was measured across the same pH range (Fig. 1). The results clearly indicated that the point of zero net charge for the protein mixture was approximately

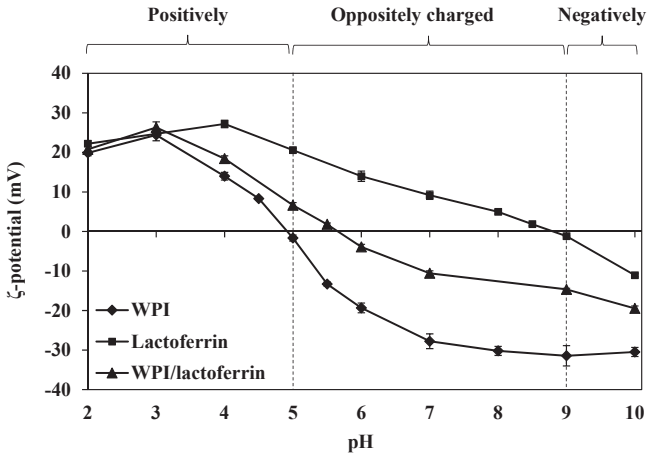


**Fig. 1.** Mean ζ-potential of 1% (w/w) protein solutions of WPI and lactoferrin and 1% (w/w) of protein mixtures of WPI and lactoferrin (1:1 ratio) at different pH values.

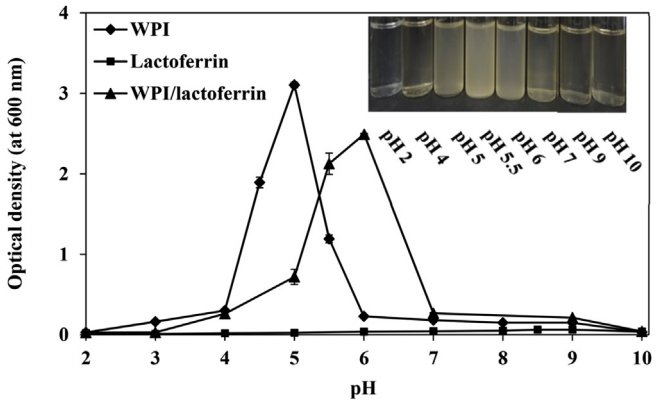


**Fig. 2.** Mean optical density (at 600 nm) of 1% (w/w) protein solutions of WPI and lactoferrin and 1% (w/w) protein mixtures of WPI and lactoferrin (1:1 ratio) at different pH values, including a photograph of the protein mixtures.

between pH 5.5 and 6 which corresponds to the pH at which the charge difference between the two individual proteins was the highest. Under these conditions, strong electrostatic interactions between the oppositely charged proteins were expected. Interactions of the two oppositely charged proteins led to the formation of complexes as evidenced by an increase in turbidity observed at pH 5.5 and 6 (Fig. 2). This corroborated with previous findings that complex coacervation of β-lactoglobulin and lactoferrin occurred in the pH range of 5.7–6.2 (Yan et al., 2013). Based on the results, all protein samples considered henceforth in this work were prepared at pH 6 to maximise the electrostatic interactions between WPI and lactoferrin.

### 3.2. Adsorption of protein bi-layers on hydrophobic surface using QCM-D

Since WPI and lactoferrin are capable of electrostatic interactions under a certain pH range, they can assemble a variety of different emulsion interfacial structures, such as single layer, bi-layer and mixed layer (Tokle et al., 2012). For example, each individual protein can form oil droplets surrounded by a single layer of protein (Fig. 3a) or different proteins can be sequentially deposited on the droplets to form bi-layer (Fig. 3b). Alternatively, the proteins may form an electrostatic complex (a mixed layer) at the interface of oil droplets (Fig. 3c). Until now, few works have reported the characteristics of protein coatings at the oil-water interface, which constitute important data for the design of interfacial structures and allow manipulation of the functionality of nanoemulsions.

As a first step, the surface adsorption and structure of protein layers on surfaces was studied by QCM-D to indirectly obtain information about the behaviour of proteins at the oil-water interface that may occur in emulsions. In our experiments, a SAM hydrophobic layer to mimic the oil-water interface in real emulsions was formed on gold surfaces. The measured contact angle of the SAM modified QCM-D sensors was 107.1 ± 0.5° indicating a hydrophobic layer was formed (contact angle of unmodified gold surface was 21.2 ± 2.3°).

The protein solutions were prepared and used in pH conditions in which they were oppositely charged. At pH 6, WPI has a negative charge of −19.3 ± 1.2 mV while the ζ-potential of lactoferrin is +14.0 ± 1.3 mV (Fig. 1). The two proteins can thus interact with each other via electrostatic interactions. The individual protein solutions were adsorbed to the gold surface to form a mono-layer and the bi-layer was formed by adding the other oppositely charged protein solution. Based on the order of protein addition, the positively charged lactoferrin molecules were adsorbed to a negatively charged WPI layer denoted as "WPI-LF" or the negatively charged WPI molecules were adsorbed to a positively charged lactoferrin layer denoted as "LF-WPI" in the experiment.

Using QCM-D, the adsorption of proteins on the modified hydrophobic surface was monitored and the frequency and dissipation shifts were recorded as a function of time. Fig. 4 reports the QCM-D results for the sequential adsorption of WPI and lactoferrin (WPI-LF sample) while Fig. 5 reports the analogous data where lactoferrin and WPI were instead sequentially adsorbed (LF-WPI sample). The qualitative trend of the two experiments was very similar, regardless of the sequence of protein loading to the QCM-D. When the first protein was fed, a rapid decrease in the frequency signal mirrored by a simultaneous dissipation increase was observed. This result is consistent with rapid adsorption of the protein molecules to the bare hydrophobic surface of the quartz sensor. Protein adsorption continued to occur at a slower rate until adsorption-desorption equilibrium was reached, as indicated by a corresponding plateau in the frequency and dissipation signals. During the first washing step with water, the frequency slightly increased while the dissipation returned back to the baseline. This condition is clearly associated with the removal of loosely bound proteins at the surface (Messina, Satriano, & Marletta, 2009). The remaining adsorbed layer consisted of protein molecules rigidly and irreversibly bound to the hydrophobic surface of the QCM-D sensor. This layer constituted a priming layer for subsequent adsorption of the oppositely charged protein. Similar phenomena were observed when the second protein solution was added and subsequently washed, i.e. an initial frequency decrease and dissipation increase during protein loading (formation of second protein layer) followed by partial frequency regain and dissipation going to zero during washing (removal of loosely viscoelastic layer of proteins and formation of a rigid irreversible layer).

The energy dissipation can be defined as the energy loss of adsorbed layer during oscillation and provides information about the viscoelastic properties of the adsorbed layer (Craig et al., 2012; Liu & Kim, 2009). It is suggested that little energy dissipation is

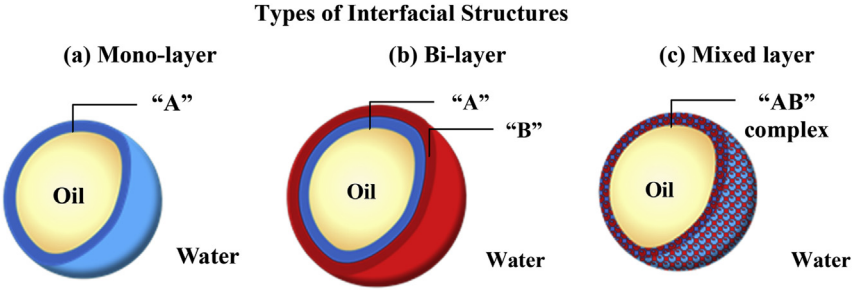


**Fig. 3.** Schematic illustrations of nanoemulsions with different interfacial structures that can be formed using two different types of proteins labelled as "A" and "B" in the diagram.

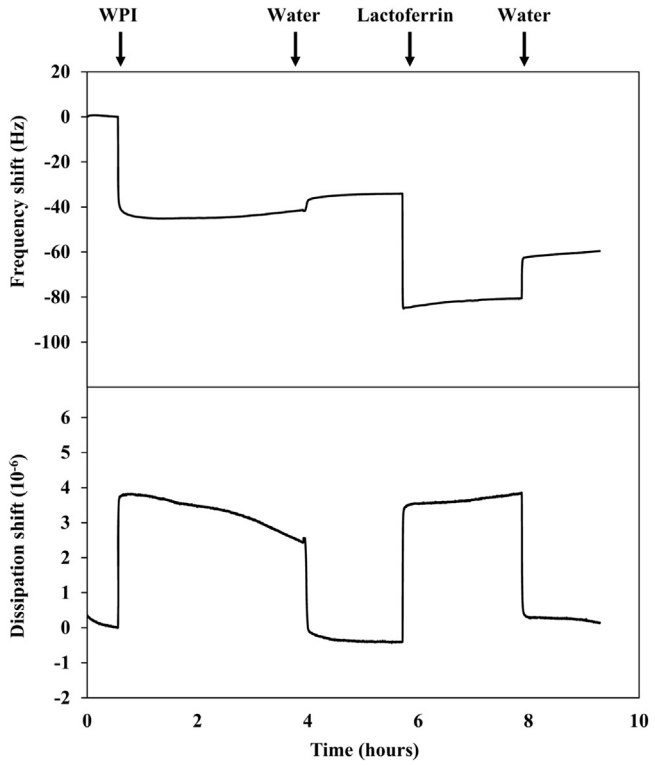


**Fig. 4.** Frequency and dissipation shift versus time at 7th overtone for the sequential adsorption of WPI first and then lactoferrin on the quartz crystal surface with alternate rinse intervals with water at pH 6.

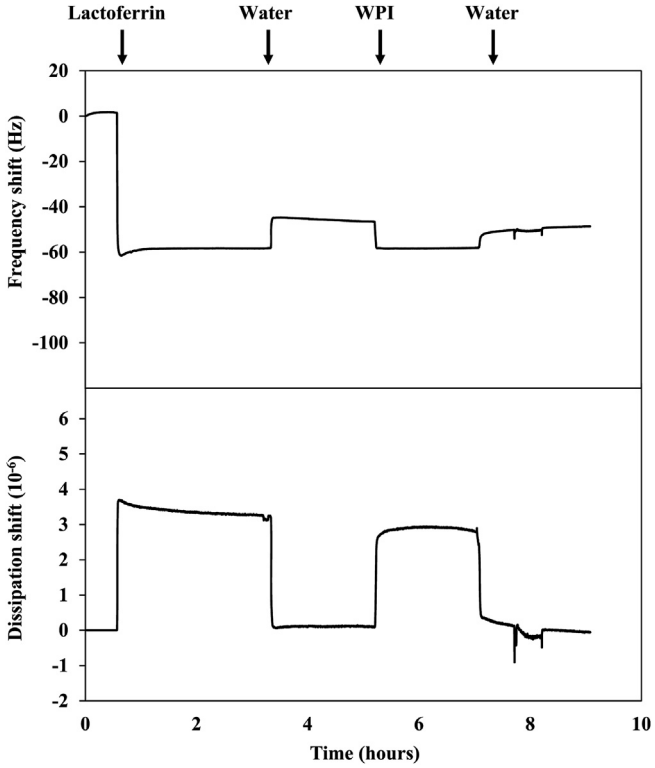


**Fig. 5.** Frequency and dissipation shift versus time at 7th overtone for the sequential adsorption of lactoferrin first and then WPI on the quartz crystal surface with alternate rinse intervals with water at pH 6.

associated to a thin, rigid film but higher energy is dissipated for a viscoelastic layer (Liu & Kim, 2009; Reviakine, Johannsmann, & Richter, 2011). While the protein solutions were initially fed into the QCM-D sensors, a relatively high dissipation signal was apparent, indicating that the adsorbed layer had a viscous component. However, this viscous layer was loosely bound and removed during rinsing, thus exposing a layer of rigidly adsorbed protein. This observation holds true for both the first and the second layer of proteins, irrespective of the order in which the proteins were fed to the sensor. Mivehi et al. (2013) proposed a trade-off of $1 \times 10^{-6}$ in the dissipation signal to distinguish between rigid and viscoelastic layers, while Reviakine et al. (2011) stated that the adsorbed layer can be assumed rigid when $\Delta D/(-\Delta f/n) << 4 \times 10^{-7}$ Hz$^{-1}$. Both conditions were satisfied for the residual protein layers following water wash, therefore the protein films were considered rigid and the adsorbed mass was calculated using the Sauerbrey model given in Equation (1).

The layer thickness of the individual proteins of WPI and lactoferrin was 4.95 and 6.97 nm, respectively (Table 1) and they are consistent with the dimensions of the proteins reported in the literature. It has been reported that whey proteins have a rigid, compact structure and β-lactoglobulin (which represents a majority of whey proteins) exists as dimers at neutral pH with a diameter of 4.8 nm based on light and X-ray scattering measurements (Baldini et al., 1999; Jost, 1993). On the other hand, the dimensions of lactoferrin based on lattice cell parameter data are ~4 × 5.1 × 7.1 nm (Mela et al., 2010). The obtained value of lactoferrin layer (6.97 nm) corresponds well to the longest axis of lactoferrin molecule, indicating that a well-formed mono-layer was adsorbed on the hydrophobic surface of the QCM-D sensor.

QCM-D results for the formation of the secondary layer were significantly different for the two bi-layers considered in this study. For WPI-LF bi-layer, a large frequency shift occurred following lactoferrin adsorption (Fig. 4), suggesting that lactoferrin molecules were deposited on the WPI-coated surface. The thickness of this secondary layer was of 5.12 nm, consistent with the size of lactoferrin molecules, leading to a bi-layer having total thickness of 10.1 nm (Table 1). In contrast, addition of WPI solution to the LF-WPI sample displayed a relatively small frequency shift, with an additional layer of 1.49 nm deposited following loading of the WPI solution. According to Trojer, Holmberg, and Nydén (2012), desorption can occur when electrostatic interactions between the adsorbed layers are weaker than hydrophobic interactions between the surface and first layer. In this case, WPI competes for the adsorption onto the hydrophobic SAM and partially displaces the previously adsorbed lactoferrin molecules, with the formation of a mixed proteinaceous layer. Similar results have been observed by Wahlgren, Arnebrant, and Paulsson (1993) using *in situ* ellipsometry at pH 7 for the sequential adsorption of lactoferrin and β-lactoglobulin (one of the main proteins in WPI) on silica surfaces. The authors in fact reported that a large amount of lactoferrin was deposited on pre-adsorbed β-lactoglobulin, but detected a decrease in the adsorbed mass when β-lactoglobulin was reversely added to a lactoferrin adsorbed layer.

### 3.3. Effect of pH on the adsorption of WPI and lactoferrin bi-layers

The stable bi-layer formed by lactoferrin molecules when deposited on WPI-coated surface was further investigated under different pH conditions. The pH of the individual proteins was precisely adjusted in the range from 2 to 10, hence spanning across the different combinations of both positively charged proteins (below pH 5), oppositely charged (between pH 5 and pH 9), and both negatively charged proteins (above pH 9). WPI was fed first to the QCM-D sensors, followed by an intermediate rinsing step with

**Table 1**
Thickness of different interfacial structures of WPI and lactoferrin adsorbed on SAM modified hydrophobic gold surface at pH 6.

| Structure | 1st Layer | | 2nd Layer | | Total thickness (nm) |
|---|---|---|---|---|---|
| | Protein type | Thickness (nm) | Protein type | Thickness (nm) | |
| Bi-layer | WPI | 4.95 ± 1.60 | Lactoferrin | 5.12 ± 0.21 | 10.1 ± 1.40 |
| | Lactoferrin | 6.97 ± 1.26 | WPI | 1.49 ± 0.21 | 8.46 ± 1.05 |
| Mixed layer | WPI/lactoferrin | 101[a] ± 33 | – | – | 101 ± 33 |

[a] Thickness achieved after loading the protein mixture for 5 h and water rinse.

water (Fig. 6a), then lactoferrin was loaded and the run was completed with a final water wash (Fig. 6b). All the solutions used in this experiment were at same pH conditions. Fig. 6b shows the frequency and dissipation shifts for the adsorption of lactoferrin on the WPI-coated surface at different pH values, while Fig. 7 presents the thickness of the second layer obtained after lactoferrin absorption.

As the investigated range of pH spanned from acidic to basic conditions, the individual protein molecules are expected to undergo some structural changes which will affect their interaction and adsorption on surfaces. Under the adsorption conditions employed, there was a larger decrease in frequency corresponding to higher protein adsorption after the addition of WPI (first layer) at pH 4 and 6 which is intermediate to the pI of WPI around 4.9 (Fig. 6b). This corresponds well with the literature on the adsorption of proteins on surfaces which in general exhibited pH dependency with a higher adsorption rate near to its pI (Belegrinou et al., 2008; Ma, Wu, & Zhang, 2013). The dominance of hydrophobic attraction is strongest at its pI with little changes in conformational structure of protein which will favour their interactions on hydrophobic gold surfaces. On the other hand, a relatively smaller decrease in frequency shift was observed in particular at pH 2 (Fig. 6a), indicating WPI adsorption was lower. This is interesting because β-lactoglobulin (a major component of whey proteins) exists as a dimer at neutral pH but can dissociate into monomers under acidic conditions (<pH 3) which can then expose hydrophobic groups (Hunt & Dalgleish, 1994; Liu & Kim, 2009). Therefore, it may be expected that hydrophobic interaction between WPI molecules and hydrophobic surface to increase at very low pH. However, WPI adsorption on the surface at pH 2 was reduced compared to at other pH levels. This can be attributed to the fact that WPI molecules were highly positive charged and electrostatic repulsion between the protein molecules was strong enough to overcome their hydrophobic attraction at the interface which can potentially reduce their alignment and intermolecular interaction on surfaces, thus less adsorption to form a less dense protein layer. This may also be related to some changes in the conformation and quaternary structure of whey protein due to pH change. For example, in a study by Zhang, Dalgleish, and Goff

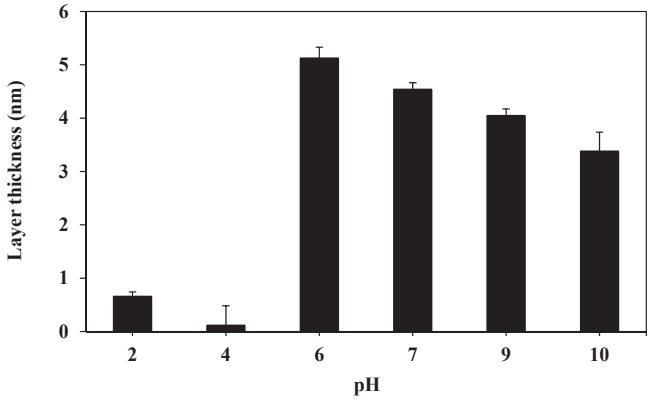


**Fig. 7.** Thickness of secondary layer after adsorption of lactoferrin on the WPI-coated surface at different pH from 2 to 10 using the Sauerbrey model.

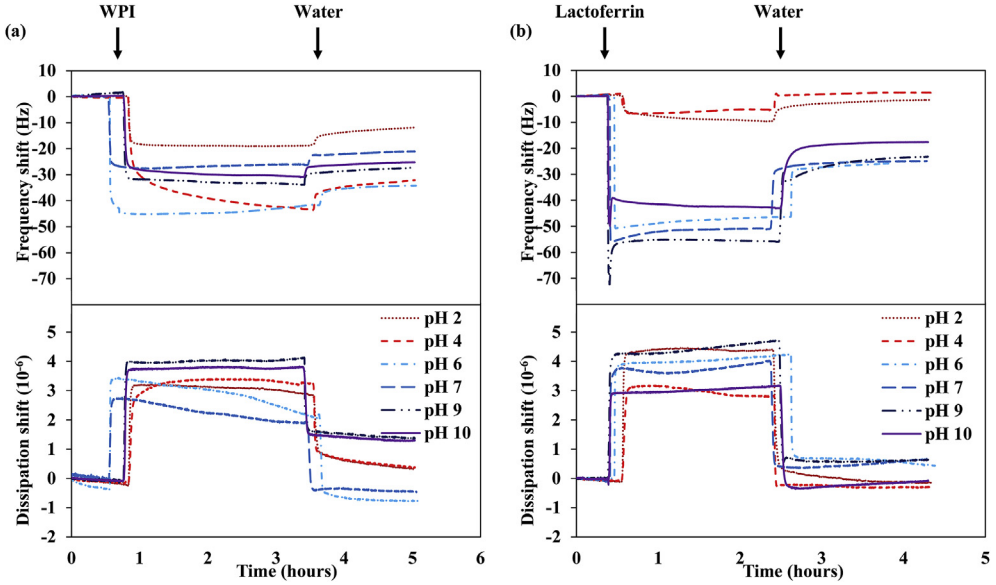


**Fig. 6.** Frequency and dissipation shift versus time at 7th overtone for (a) the adsorption of WPI on the quartz crystal surface (first layer) and (b) the adsorption of lactoferrin on the WPI-coated quartz crystal surface (second layer) at various pHs.

(2004) that reported protein adsorption to air/water interfaces in aqueous foam, β-lactoglobulin is described to be less competitive to interfacial adsorption at pH 3 due to its becoming more rigid and thermodynamically stable at low pH.

In the second stage of the adsorption, lactoferrin molecules were added to the WPI-coated surface under the same pH conditions. At pH 2 and 4, the frequency remained practically at the baseline of WPI (Fig 6b), indicating that there was no adsorption of lactoferrin on the WPI layer, mainly because of charge repulsion between the two positively charged proteins. At pH 6 or higher, the frequency shift was significant, indicating the adsorption of lactoferrin molecules on top of the WPI-coated surface. Interestingly, the thickness of this secondary layer of lactoferrin slightly decreased as the pH further increased above pH 6 (Fig. 7). This result is consistent with the large but opposite charge densities on the two proteins studied at pH 6 (Fig. 1), with electrostatic interactions playing the strongest role at this pH. Interestingly, there was still a considerable amount of lactoferrin adsorbing to the WPI-coated surfaces at pH equal or higher than 9 (Fig. 7). Lactoferrin is a large globular protein which displays a bipolar charge distribution (Mantel, Miyazawa, & Broxmeyer, 1994). Therefore, the protein presents positively charged patches even at the pI or above (Iafisco, Foggia, Bonora, Prat, & Roveri, 2011; Müller, 2014). In addition, the interactions between lactoferrin and WPI can be enhanced by other interaction forces such as hydrophobic attractions and hydrogen bonds which tend to dominate near the pI (McClements, 1999). This result is consistent with the study on adsorption of lactoferrin on negatively charged adsorbents at different pH and salt concentrations (Du, Lin, Wang, & Yao, 2014). The authors reported that there was substantial amount of lactoferrin adsorbed even at pH near the pI of lactoferrin.

### 3.4. Adsorption of protein complex on hydrophobic surface using QCM-D

The adsorption behaviour of a protein mixture of WPI and lactoferrin was very different to that previously observed with sequential adsorption of the two proteins. The adhered layers displayed relatively large frequency and dissipation shifts and showed no trend of reaching saturation or equilibrium after 5 h exposure to the protein mixture (Fig. 8). This could be due possibly to a feature of continuous sedimentation associated with large aggregates of protein complex of WPI and lactoferrin at pH 6 as indicated in Table 1 and Fig. 2. The layer formed was however stable against rinsing with water, indicating relatively strong cohesive interactions.

According to the high dissipation value measured for the adsorption of protein complex, the Kevin-Voigt model was used to estimate the thickness of the adsorbed film at the end of the experiment (Table 1). This thickness is to be considered an indicative measure only, because of the limitations of the Voigt model to describe such thick layers, and also because the layer did not reach an equilibrium value. The formed layer had a thickness of 101 μm, much larger than what was obtained when sequentially loading the two pure proteins in bi-layers, and potentially could have further increased after continuous loading of the protein mixture. This observation, together with the negligible desorption of proteins during the rinsing step, additionally indicates the formation of a strong cohesive adsorbed layer with the two proteins mutually interacting. The complex proteinaceous layer was formed by a mixture of WPI and lactoferrin at pH 6, where the opposite electrical charges on the proteins are fostering a strong durable layer. The consequent aggregation and unfolding of the two proteins lead to establishment of additional hydrophobic, hydrogen bonding as well as some dipole-dipole and charge-dipole interactions, with the

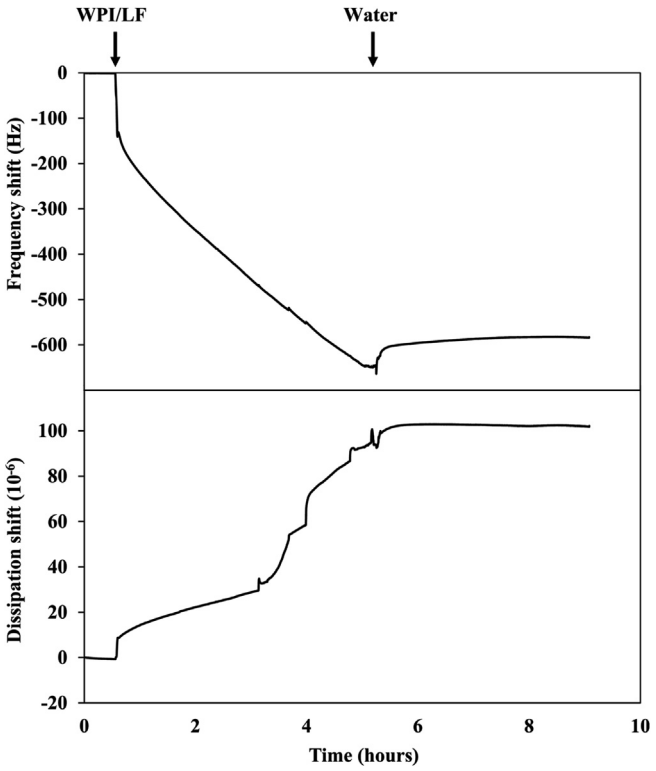


**Fig. 8.** Frequency and dissipation shift versus time at 7th overtone for the adsorption of protein complex of WPI and lactoferrin on the quartz crystal surface with water rinse after 5 h at pH 6.

consequent formation of stable electrically neutral adsorbed layer of proteins (Ye, 2008). These non-electrostatic attractive forces can act in concert offering a large driving force for the continued adsorption of the protein complex on the sensor surface and formed a thick layer.

To gain more information on the adsorption behaviour, dissipation shift was plotted as a function of frequency shift (Fig. 9). In such a plot, a relatively small slope (i.e. small dissipation gain for a given frequency shift) characterises rigidly adsorbed layers, while a larger slope (i.e. high dissipation for a given frequency shift) is representative of a soft viscoelastic layer (Belegrinou et al., 2008). Based on the results reported in Fig. 9, the mixed protein layer

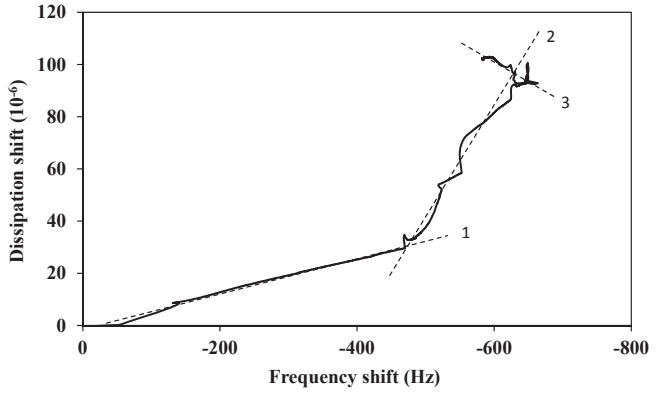


**Fig. 9.** Dissipation shift versus frequency shift plot at 7th overtone during the adsorption of protein complex of WPI and lactoferrin at pH 6. Line 1: trend line during adsorption of initial layer. Line 2: trend line during formation of secondary soft layer. Line 3: rinse step with water.

**Table 2**
Mean droplet size and ζ-potential of emulsions containing different interfacial structures at pH 6.

| Emulsion type | Mean particle diameter (nm) | Mean PDI/Span | Mean ζ-potential (mV) |
|---|---|---|---|
| **WPI** | 78.4[a] ± 1.8 | 0.21 ± 0.01 | −26.3 ± 1.3 |
| **Lactoferrin** | 94.2[a] ± 5.5 | 0.18 ± 0.01 | +20.0 ± 0.8 |
| **WPI-lactoferrin** | 90.1[a] ± 4.7 | 0.23 ± 0.02 | +1.3 ± 0.3 |
| **Lactoferrin-WPI** | 15759[b] ± 5386 | 1.37 ± 0.01 | −2.4 ± 1.1 |
| **WPI/lactoferrin mixed** | 22291[b] ± 2650 | 2.07 ± 0.11 | −7.7 ± 0.5 |

[a] Particle size of nanoemulsions stabilised by WPI, lactoferrin and WPI-lactoferrin is reported as Z-average mean diameter using a Malvern Zetasizer Nano ZS.
[b] Particle size of lactoferrin-WPI emulsion and WPI/lactoferrin mixed layer emulsion is reported as the volume mean diameter ($D_{43}$) measured using a Mastersizer 2000.

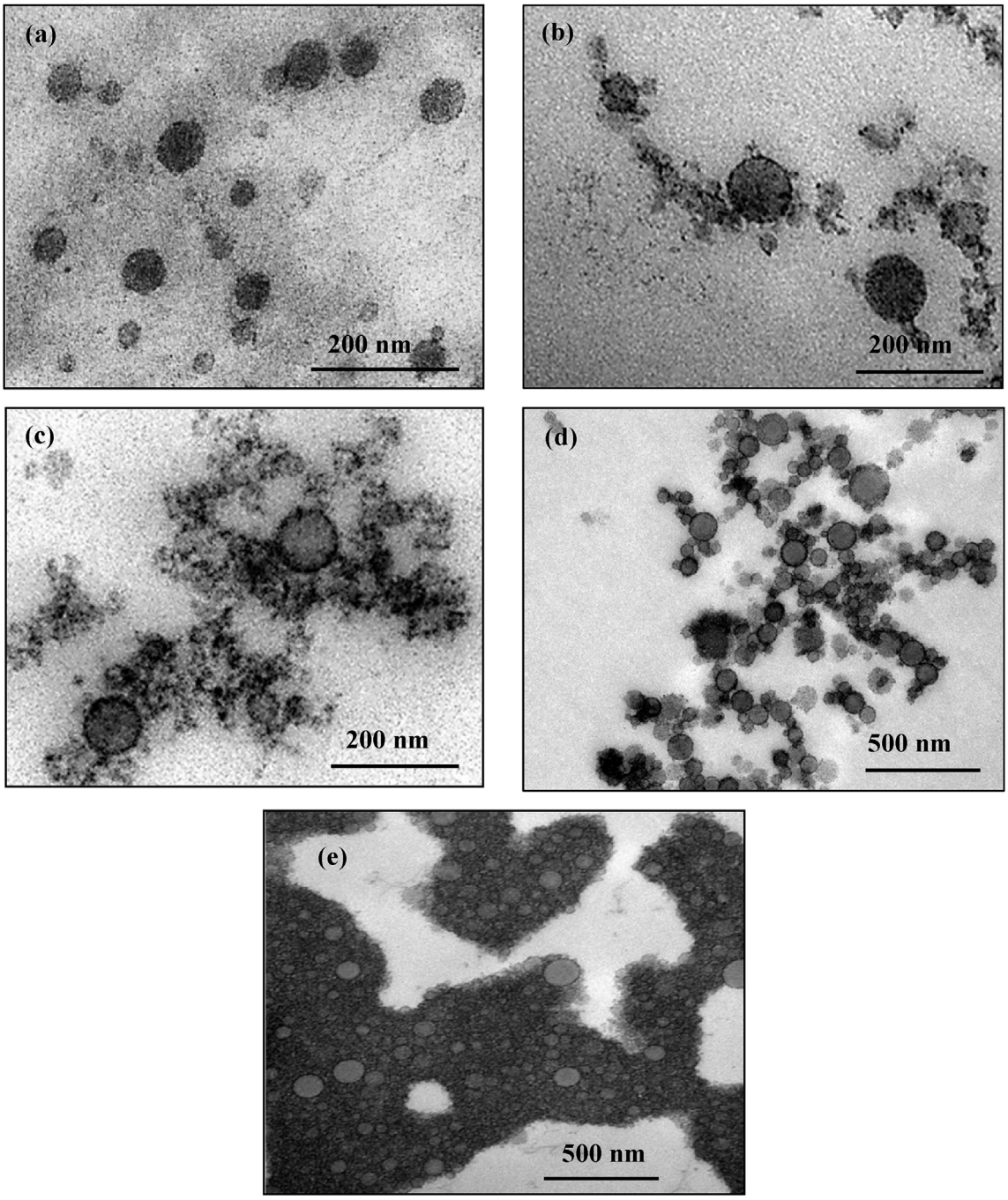


**Fig. 10.** TEM images of nanoemulsions with different interfacial structures (0.5% w/w oil) of (a) WPI mono-layer, (b) Lactoferrin mono-layer, (c) WPI-lactoferrin bi-layer, (d) Lactoferrin-WPI bi-layer and (e) WPI/lactoferrin mixed layer.

initially deposited onto the sensor was rigidly coupled to the hydrophobic surface, but progressive deposition produced a softer second layer having more viscous structure which might be expected due to retention of water as the protein film was continuously deposited on the surface. It is important to note that there is the possibility that the secondary adsorption observed (line 2 in Fig. 2) could also be possibly related to continuous sedimentation of large aggregates of the mixed proteins described above.

The thickness of this mixed protein layer was 10 times larger than the one measured for the protein bi-layer. It is worth noticing that the layer thickness of the protein bi-layers approximately corresponded to the sum of the two stacked mono-layers for the individual proteins, whereas the mixture of proteins formed a thick multi-layer of protein complex. Preliminary results confirmed that the thickness of the bi-layer can be further increased by sequential addition of the oppositely charged proteins, leading to film with larger thicknesses than the simple bi-layer. However these experiments are not part this current study and will be discussed more in details in the future.

### 3.5. Formation of nanoemulsions with different interfacial structures

Nanoemulsions with different interfacial structures were formed using a combination of emulsification and solvent evaporation. All the nanoemulsions were prepared at pH 6 as the magnitude of the net opposite charge between WPI and lactoferrin was highest at this pH. The nanoemulsions stabilised by WPI or lactoferrin (single layer) were relatively small (<100 nm) and with electrical characteristics consistent with the charge of the proteins (Table 2). At pH 6, the WPI-stabilised primary emulsion droplets were negatively charged ($-26.3 \pm 1.3$ mV) while the ones stabilised by lactoferrin were positively charged ($+20.0 \pm 0.8$ mV).

Sequential adsorption of lactoferrin onto WPI-stabilised primary nanoemulsions lead to an increase in droplet size of around 11.7 nm in diameter, consistent with the formation of a stable bi-layer where the second layer had a thickness of around 5.8 nm. This result is very similar to what previously obtained in the QCM-D experiments (Table 1). The TEM images revealed that the singly WPI-coated or lactoferrin-coated oil droplets seem to have a relatively thin layer surrounding the oil droplets (Fig. 10a and b) although this is not seen clearly. However, a thicker layer (presumably protein) seems to form in bi-layer nanoemulsions of WPI and lactoferrin with some flocs (Fig. 10c and d). The good stability of WPI-stabilised nanoemulsions coated by lactoferrin suggested that lactoferrin molecules on the outer layer provide a strong steric hindrance arising from the carbohydrate side chains on the lactoferrin molecules (Tokle et al., 2012).

On the other hand, nanoemulsions with lactoferrin in the first monolayer became unstable and formed large aggregates upon addition of the WPI solution. In fact, the ζ-potential of the resulting droplets was close to neutrality, providing little electrostatic repulsion to overcome the attractive forces of hydrophobic interaction for droplet aggregation. As a result, the droplet size of this secondary emulsion was very large ($D_{43}$ ~$15 \pm 5.4$ μm), and emulsion flocs appeared in the TEM image of LF-WPI nanoemulsions (Fig. 10d). This result is again consistent with the QCM-D results, where the LF-WPI experiment was characterized by the competitive displacement of lactoferrin by the incoming WPI, producing a mixed layer containing both proteins. Accordingly, it is reasonable to assume the overall charge displayed by the resulting droplet is near neutral (Table 2).

Nanoemulsions treated with the protein complex containing a mixture of WPI and lactoferrin at pH 6 produced a poorly stable emulsion which led to phase separation. This is confirmed by the TEM images which showed a large aggregated mass of proteins surrounding the droplets (Fig. 10e). This observation is again in good agreement with the QCM-D results, where the protein complexes were continuously adsorbed to the sensor surface indicating a high tendency for protein aggregation to occur. In addition, the protein complex adsorbed to the surface of oil droplets will be constituted by unfolded or partially folded proteins, whose hydrophobic groups are exposed, hence further promoting proteins aggregation and engulfment of the droplets.

## 4. Conclusions

In this study, the properties of nanoemulsions with different interfacial configurations composed of WPI and lactoferrin were investigated in line with QCM-D to understand the mechanism underlying their interactions at droplet interface using a simulated model on hydrophobic surfaces. It was found that nanoemulsions stabilised with a bi-layer structure of WPI and lactoferrin were more stable than those formed by lactoferrin and WPI or a mixture of the two proteins at pH 6. On the contrary, nanoemulsions formed by protein complex caused droplet aggregation as a result of attractive interactions between the adsorbed layers of the droplets. This finding is in agreement with the QCM-D data obtained for the adsorption of different interfacial structures of proteins on a modified hydrophobic surface. The QCM-D results showed that there was protein adsorption when the protein layers were added to a surface pre-coated by another protein to form a thin layer via electrostatic interactions. However, the protein complex formed a thick, viscous layer that was strongly attached to the surfaces. This research provided in depth understanding of the formation of stable nanoemulsions with different interfacial structures.

## Acknowledgements

This study was funded by the Royal Society of New Zealand (KOR-MAU1101) under New Zealand - Korea International Research Programme (Food Innovation). The authors would like to thank Jordan Taylor, Manawatu Microscopy and Imaging Centre, Massey University for her assistance in TEM analysis.

## References

Baker, E. N., & Baker, H. M. (2005). Molecular structure, binding properties and dynamics of lactoferrin. *Cellular and Molecular Life Sciences, 62*(22), 2531–2539.

Baldini, G., Beretta, S., Chirlco, G., Franz, H., Maccioni, E., Mariani, P., et al. (1999). Salt-induced association of β-lactoglobulin by light and X-ray scattering. *Macromolecules, 32*(19), 6128–6138.

Belegrinou, S., Mannelli, I., Lisboa, P., Bretagnol, F., Valsesia, A., Ceccone, G., et al. (2008). pH-dependent immobilization of proteins on surfaces functionalized by plasma-enhanced chemical vapor deposition of poly(acrylic acid)- and poly(-ethylene oxide)-like films. *Langmuir, 24*(14), 7251–7261.

Berendsen, R., Güell, C., Henry, O., & Ferrando, M. (2014). Premix membrane emulsification to produce oil-in-water emulsions stabilized with various interfacial structures of whey protein and carboxymethyl cellulose. *Food Hydrocolloids, 38*, 1–10.

Boddohi, S., Almodóvar, J., Zhang, H., Johnson, P. A., & Kipper, M. J. (2010). Layer-by-layer assembly of polysaccharide-based nanostructured surfaces containing polyelectrolyte complex nanoparticles. *Colloids and Surfaces B: Biointerfaces, 77*(1), 60–68.

Bouyer, E., Mekhloufi, G., Rosilio, V., Grossiord, J. L., & Agnely, F. (2012). Proteins, polysaccharides, and their complexes used as stabilizers for emulsions: alternatives to synthetic surfactants in the pharmaceutical field? *International Journal of Pharmaceutics, 436*(1–2), 359–378.

Chandrasekaran, N., Dimartino, S., & Fee, C. (2013). Study of the adsorption of proteins on stainless steel surfaces using QCM-D. *Chemical Engineering Research and Design, 91*(9), 1674–1683.

Craig, M., Bordes, R., & Holmberg, K. (2012). Polypeptide multilayer self-assembly and enzymatic degradation on tailored gold surfaces studied by QCM-D. *Soft Matter, 8*(17), 4788–4794.

Du, Q., Lin, D., Wang, R., & Yao, S. (2014). Mechanistic analysis of effects of pH and salt concentration on lactoferrin adsorption onto adsorbents with sulfonic ligand. *Chemical Industry and Engineering Society of China, 65*(2), 593–598.

Gallier, S., Tate, H., & Singh, H. (2013). In vitro gastric and intestinal digestion of a walnut oil body dispersion. *Journal of Agricultural and Food Chemistry, 61*(2), 410–417.
Guzey, D., & McClements, D. J. (2006). Formation, stability and properties of multilayer emulsions for application in the food industry. *Advances in Colloid and Interface Science, 128–130*, 227–248.
Höök, F., Kasemo, B., Nylander, T., Fant, C., Sott, K., & Elwing, H. (2001). Variations in coupled water, viscoelastic properties, and film thickness of a Mefp-1 protein film during adsorption and cross-linking: a quartz crystal microbalance with dissipation monitoring, ellipsometry, and surface plasmon resonance study. *Analytical Chemistry, 73*(24), 5796–5804.
Hunt, J. A., & Dalgleish, D. G. (1994). Effect of pH on the stability and surface composition of emulsions made with whey protein isolate. *Journal of Agricultural and Food Chemistry, 42*(10), 2131–2135.
Iafisco, M., Foggia, M. D., Bonora, S., Prat, M., & Roveri, N. (2011). Adsorption and spectroscopic characterization of lactoferrin on hydroxyapatite nanocrystals. *Dalton Transactions, 40*(4), 820–827.
Ito, E., Arai, T., Hara, M., & Noh, J. (2009). Surface potential change depending on molecular orientation of hexadecanethiol self-assembled monolayers on AU(111). *Bulletin of the Korean Chemical Society, 30*(6), 1309–1312.
Jost, R. (1993). Functional characteristics of dairy proteins. *Trends in Food Science & Technology, 4*(9), 283–288.
Krivosheeva, O., Dėdinaitė, A., & Claesson, P. M. (2012). Adsorption of Mefp-1: Influence of pH adsorption kinetics and adsorbed amount. *Journal of Colloid and Interface Science, 379*(1), 107–113.
Lebec, V., Landoulsi, J., Boujday, S., Poleunis, C., Pradier, C.-M., & Delcorte, A. (2013). Probing the orientation of β-lactoglobulin on gold surfaces modified by alkyl thiol self-assembled monolayers. *The Journal of Physical Chemistry, 117*(22), 11569–11577.
Lee, S. J., Choi, S. J., Li, Y., Decker, E. A., & McClements, D. J. (2011). Protein-stabilized nanoemulsions and emulsions: comparison of physicochemical stability, lipid oxidation, and lipase digestibility. *Journal of Agricultural and Food Chemistry, 59*(1), 415–427.
Lee, S. J., & McClements, D. J. (2010). Fabrication of protein-stabilized nanoemulsions using a combined homogenization and amphiphilic solvent dissolution/evaporation approach. *Food Hydrocolloids, 24*(6–7), 560–569.
Liu, S. X., & Kim, J. T. (2009). Application of Kevin-Voigt model in quantifying whey protein adsorption on polyethersulfone using QCM-D. *Journal of Laboratory Automation, 14*(4), 213–220.
Lundin, M., Elofsson, U. M., Blomberg, E., & Rutland, M. W. (2010). Adsorption of lysozyme, β-casein and their layer-by-layer formation on hydrophilic surfaces: effect of ionic strength. *Colloids and Surfaces B: Biointerfaces, 77*(1), 1–11.
Malmström, J., Agheli, H., Kingshott, P., & Sutherland, D. S. (2007). Viscoelastic modelling of highly hydrated laminin layers at homogenous and nanostructured surfaces: quantification of protein layer properties using QCM-D and SPR. *Langmuir, 23*(19), 9760–9768.
Mantel, C., Miyazawa, K., & Broxmeyer, H. E. (1994). Physical characteristics and polymerization during iron saturation of lactoferrin, a myelopietic regulatory molecule with suppressor activity. *Advance in Experimental Medicine and Biology, 357*, 121–132.
Mao, L., Boiteux, L., Roos, Y. H., & Miao, S. (2014). Evaluation of volatile characteristics in whey protein isolate-pectin mixed layer emulsions under different environmental conditions. *Food Hydrocolloids, 41*, 79–85.
Ma, C., Wu, B., & Zhang, G. (2013). Protein-protein resistance investigated by quartz crystal microbalance. *Colloids and Surface B: Biointerfaces, 104*, 5–10.
McClements, D. J. (1999). *Food emulsions principles, practices, and techniques*. Boca Raton, FL: CRC Press.
McClements, D. J., & Rao, J. (2011). Food-grade nanoemulsions: formulation, fabrication, properties, performance, biological fate, and potential toxicity. *Critical Reviews in Food Science and Nutrition, 51*(4), 285–330.
Mela, I., Aumaitrem, E., Williamson, A., & Yakubov, G. E. (2010). Charge reversal by salt-induced aggregation in aqueous lactoferrin solutions. *Colloids and Surfaces B: Biointerfaces, 78*(1), 53–60.
Messina, G. M. L., Satriano, C., & Marletta, G. (2009). A multitechnique study of preferential protein adsorption on hydrophobic and hydrophilic plasma-modified polymer surfaces. *Colloids and Surfaces B: Biointerfaces, 70*(1), 76–83.
Mivehi, L., Bordes, R., & Holmberg, K. (2013). Adsorption of cationic gemini surfactants at solid surfaces studied by QCM-D and SPR-effect of the presence of hydroxyl groups in the spacer. *Colloids and Surfaces A: Physicochemical and Engineering Aspects, 419*, 21–27.
Müller, M. (2014). *Polyelectrolyte complexes in the dispersed and solid state II: Application aspects*. Springer-Verlag Berlin Heidelberg.
Nováková, Z., Oriňáková, R., Oriňák, A., Hvizdoš, P., & Fedorková, A. S. (2014). Elimination voltammetry as a new method for studying the SAM formation. *Internal Journal of Electrochemical Science, 9*(7), 3846–3863.
Pallandre, S., Decker, E. A., & McClements, D. J. (2007). Improvement of stability of oil-in-water emulsions containing caseinate-coated droplets by addition of sodium alginate. *Journal of Food Science, 72*(9), E518–E524.
Reviakine, I., Johannsmann, D., & Richter, R. P. (2011). Hearing what you cannot see and visualizing what you hear: interpreting quartz crystal microbalance data from solvated interfaces. *Analytical Chemistry, 83*(23), 8838–8848.
Salminen, H., & Weiss, J. (2013). Effect of pectin type on association and pH stability of whey protein-pectin complexes. *Food Biophysics, 9*(1), 29–38.
Sarkar, A., Goh, K. K. T., Singh, R. P., & Singh, H. (2009). Behaviour of an oil-in-water emulsion stabilized by β-lactoglobulin in an in vitro gastric model. *Food Hydrocolloids, 23*(6), 1563–1569.
Sauerbrey, G. (1959). The use of quartz crystals for weighing thin layers and for microweighing. *Zeitschrift für Physik, 155*(2), 206–222.
Skirtach, A. G., Yashchenok, A. M., & Möhwald, H. (2011). Encapsulation, release and applications of LBL polyelectrolyte multilayer capsules. *Chemical Communications, 47*, 12736–12746.
Steijns, J. M., & van Hooijdonk, A. C. M. (2000). Occurrence, structure, biochemical properties and technological characteristics of lactoferrin. *British Journal of Nutrition, 84*(1), S11–S17.
Sukhorukov, B., Caruso, F., Davis, S. A., & Möhwald, H. (1998). Novel hollow polymer shells by colloid-templated assembly of polyelectrolytes. *Angewandte Chemie International Edition, 37*(16), 2201–2205.
Tiwari, R., & Takhistove, P. (2012). Nanotechnology-enabled delivery systems for food functionalization and fortification. In G. W. Padua, & Q. Wang (Eds.), *Nanotechnology research methods for foods and bioproducts* (pp. 55–101). John Wiley & Sons, Inc.
Tokle, T., Decker, E. A., & McClements, D. J. (2012). Utilisation of interfacial engineering to produce novel emulsion properties: pre-mixed lactoferrin/β-lactoglobulin protein emulsifiers. *Food Research International, 49*(1), 46–52.
Trojer, M. A., Holmberg, K., & Nydén, M. (2012). The importance of proper anchoring of an amphiphilic dispersant for colloidal stability. *Langmuir, 28*(9), 4047–4050.
Trojer, M. A., Mohamed, A., & Eastoe, J. (2013). A highly hydrophobic anionic surfactant at oil–water, water–polymer and oil–polymer interfaces: implications for spreading coefficients, polymer interactions and microencapsulation via internal phase separation. *Colloids and Surfaces A: Physicochemical and Engineering Aspects, 436*, 1048–1059.
Trojer, M. A., Nordstiema, L., Nordin, M., Nydén, M., & Holmberg, K. (2013). Encapsulation of actives for sustained release. *Physical Chemistry Chemical Physics, 15*(41), 17727–17741.
Trojer, M. A., Nordstierna, L., Bergek, J., Blanck, H., Holmberg, K., & Nydén, M. (2015). Use of microcapsules as controlled release devices for coatings. *Advances in Colloid and Interface Science, 222*, 18–43.
Voinova, M. V., Rohahl, M., Jonson, M., & Kasemo, B. (1999). Viscoelastic acoustic response of layered polymer films at fluid solid interfaces: continuum mechanics approach. *Physica Scripta, 59*(5), 391–396.
Wahlgren, M. C., Arnebrant, T., & Paulsson, M. A. (1993). The adsorption from solutions of β-lactoglobulin mixed with lactoferrin or lysozyme onto silica and methylated silica surfaces. *Journal of Colloid and Interface Science, 158*(1), 46–53.
Weiss, J., Gaysinsky, S., Davidson, P. M., & McClements, D. J. (2009). Nanostructured encapsulation systems: food antimicrobials. In G. Barbosa-Canovas, A. Mortimer, D. Lineback, W. Spiess, K. Buckle, & P. Colonna (Eds.), *Global issues in food science and technology* (pp. 435–479). Academic Press.
Yan, Y., Kizilay, E., Seeman, D., Flanagan, S., Dubin, P. L., Bovetto, L., et al. (2013). Heteroprotein complex coacervation: bovine β-lactoglobulin and lactoferrin. *Langmuir, 29*(50), 15614–15623.
Ye, A. (2008). Complexation between milk proteins and polysaccharides via electrostatic interaction: principles and application - a review. *International Journal of Food Science and Technology, 43*(3), 406–415.
Ye, A., & Singh, H. (2007). Formation of multilayers at the interface of oil-in-water emulsion via interactions between lactoferrin and β-lactoglobulin. *Food Biophysics, 2*(4), 125–132.
Zhang, Z., Dalgleish, D. G., & Goff, H. D. (2004). Effect of pH and ionic strength on competitive protein adsorption to air/water interfaces in aqueous foams made with mixed milk proteins. *Colloids and Surfaces B: Biointerfaces, 34*, 113–121.